Structural Characterization and Antidepressant-Like Effects of *Polygonum sibiricum* Polysaccharides Associated with Regulating Microglial Polarization in Cums-Induced Zebrafish

Ying yu Zhang , Dan yang Wang , Jia meng Liu , Ya juan Bai , Bei Fan , Cong Lu * , Feng zhong Wang *

Posted Date: 27 December 2023

doi: 10.20944/preprints202312.2054.v1

Keywords: depression; Polygonati Rhizoma polysaccharides; microglia polarization

Article

Structural Characterization and Antidepressant-like Effects of *Polygonum sibiricum* Polysaccharides Associated with Regulating Microglial Polarization in CUMS-Induced Zebrafish

Yingyu Zhang [1], Danyang Wang [1], Jiameng Liu [1], Yajuan Bai [1,2], Bei Fan [1,2], Cong Lu [1,2,*] and Fengzhong Wang [1,2,*]

[1] Institute of Food Science and Technology, Chinese Academy of Agricultural Sciences (CAAS), Beijing 100193, China
[2] Sanya Institute, Hainan Academy of Agricultural Sciences, Sanya 572025, China
* Correspondence: lucong198912@126.com (C.L.), wangfengzhong@sina.com (F.W.); Tel: +86-10-62810295; Fax: +86-10-62810295.

Abstract: Background: The polysaccharides are one of the main active ingredients of *Polygonum sibiricum* (PSP), which is a traditional food and medicine homologues in China. The antidepressant-like effects of PSP and its underlying mechanisms remain to be studied in depth, especially the regulation of microglial polarization. Methods: The chemical composition and structural characteristics of PSP was determined firstly. The CUMS procedure was carried out to the zebrafish for 5 weeks and PSP were immersed administration for 9 days (1 h/d). The body weight of zebrafish was monitored and the behavioral tests, including the novel tank test and light and dark tank test, were performed to evaluate the antidepressant-like effects of PSP. Then the function of HPI axis, the levels of peripheral inflammation, neuronal and blood-brain barrier damage in mesencephalon and telencephalon and the mRNA expression of M1/M2 phenotype genes in brain were examined. Results: PSP samples had the typical structure characteristics of polysaccharide, consisting of glucose, mannose and galactose with the average Mw 20.48 kDa, which owned a porous and agglomerated morphology. Compared with untreated zebrafish, the depression-like behaviors of CUMS-induced zebrafish were significantly attenuated. PSP significantly decreased the levels of cortisol and the pro-inflammatory cytokines and increased the levels of the anti-inflammatory cytokines in the body of CUMS-induced depressive zebrafish. Furthermore, neuronal and blood-brain barrier damage in mesencephalon and telencephalon and the mRNA expression of M1/M2 phenotype genes in brain were remarkably reversed by PSP. Conclusion: These findings indicated that the antidepressant-like effects of PSP were related to alter the HPI axis hyperactivation, suppress peripheral inflammation, inhibit neuroinflammation induced by microglia hyperactivation, and modulate microglial M1/M2 polarization. The current study provides foundation to the future exploitation of PSP in the functional foods of emotional regulation.

Keywords: depression; *Polygonati Rhizoma* polysaccharides; microglia polarization

1. Introduction

Depression has become one of the most common types of psychological disorders, characterized by prolonged depressed mood, especially in the outbreak of new coronavirus and post-epidemic era environment, which severely limits people's psychosocial abilities and reduces the quality of life (Deng et al., 2021). Chemically synthesized drugs are the main clinical drugs currently used for depression, which not only take longer to produce efficacy, but also are accompanied by severe and serious side effects such as sudden weight loss, anorexia and insomnia, making their safety a potential problem and limiting their clinical application (Moret et al., 2009). In the context of healthy

 doi:10.20944/preprints202312.2054.v1

China, combined with the national demand of 'Healthy China 2030 Plan', and with the upgrading of the consumption structure and demand for nutrition and health, functional foods of emotional health are in robust demand (Gao et al., 2021). It is especially important to develop the health products with the high antidepressant effects to prevent and treat depression.

Neuroinflammation is considered as a pathological mechanism of depression. Microglia are key members of the immune defense in the central nervous system (CNS), which plays a central role in immunity and inflammation (Cao et al., 2022). When homeostasis is disturbed, microglia can be rapidly activated. The activated microglia have a "double-edged" effect, manifesting themselves in two polarized phenotypes: a classically activated M1 and an alternatively activated M2 phenotype. M1 microglia are associated with excessive release of pro-inflammatory factors that can exacerbate inflammatory damage in the CNS and lead to neurotrophic dysfunction, while M2 microglia are associated with the secretion of anti-inflammatory and neurotrophic factors that can help to antagonize inflammatory damage and promote recovery and remodeling of neural tissue (Guo et al.,2022). One of the potential therapeutic targets for depression is regulating M1/M2 polarization of microglia, so as to dynamically regulate neuroinflammation and maintain homeostasis.

Polygonum sibiricum (PS) is a traditional food and medicine homologues in China. *Polygonum sibiricum* polysaccharides (PSP) is one of the main active components of it, which is almost nontoxic and has rarely negative effects, making it potentially useful in health care and food industry. In previous studies, PSP showed antidepressant effects in both lipopolysaccharide-induced and the chronic unpredictable mild stress (CUMS)-induced depressive mice models. Regulation of the hypothalamic-pituitary-adrenal (HPA) axis dysfunction, neurotransmitters (5-HT and NE) levels, neuroinflammation, gut microbiota composition and short-chain fatty acids levels were the antidepressant mechanisms involved (Shen et al., 2021; Shen et al., 2022; Zhang et al., 2023; Zhang et al., 2023). However, the mechanisms remain to be studied in depth, especially for that whether PSP can show the antidepressant-like effects by inhibiting microglia activation and regulate the M1/M2 phenotype of microglia.

Therefore, the depressive model in zebrafish was established by the chronic unpredictable mild stress for 5 weeks, then the antidepressant-like effects and the modulatory effects on microglia of PSP in CUMS-induced zebrafish were evaluated by analyzing body weight, depressive-like behaviors in novel tank test (NTT), light and dark tank test (LDT), hypothalamic-pituitary-interrenal axis (HPI), peripheral inflammation, structure of neuron and blood-brain barrier (BBB), activation state of microglia, and M1/M2 phenotype markers. Hopefully, the present study can provide the theoretical foundation for the development of emotional regulation products and application of PSP in the wellness industry.

2. Materials and methods

2.1. Animals, materials and reagents

Adult wild type zebrafish (4–6 months of age) were obtained from aquarium (Ornamental fish supplier, Beijing, China). The animals were maintained at 27 ℃ in filtered system water (pH = 7.0–7.6) with light (14 h)-dark (10 h) cycle, according to standards. All animals received fresh Artemia twice daily, unless indicated otherwise in the CUMS procedure. Animal experimentation fully comply with National and institutional guidelines and regulations, and was approved by the ethics committee for research on laboratory animal use of the institution.

PSP was obtained from Shanghai Yuanye Bio-Technology Co., Ltd. (Shanghai, China). Fluoxetine hydrochloride (FLU) was purchased from MedChemExpress LLC. Commercial sandwich enzyme-linked immunosorbent assay (ELISA) kits for cortisol (CORT), tumor necrosis factor (TNF-α), interleukin (IL)-6, IL-1β and IL-10 were obtained from Jianglai Biological Technology Co., Ltd. (Shanghai, China). qRT-PCR primers from Tsingke Biotechnology Co., Ltd. (Beijing, China). Toluidine blue O were obtained from Wuhan servicebio technology Co., Ltd. (Wuhan, China). DAB kit from Epsilon Biotechnology Co., Ltd., (Beijing, China). All other reagents were of analytical grade.

 doi:10.20944/preprints202312.2054.v1

2.2. Structure characterization of PSP

2.2.1. Determination of content of total carbohydrate, protein, phenols, flavonoids, crude fat, ash and water

The contents of total carbohydrates, protein, phenols, flavonoids, crude fat, ash were quantified by the phenol-sulfuric acid method (DuBois et al., 1956), the bicinchoninic acid method (Walker, 1994), the Folin-ciocalteu method, the NaNO2-Al(NO3)3-NaOH colorimetric method (Bao, Li, Zheng, & Li, 2015), the Soxhlet extraction method and carbonization method (Vegh et al., 2022), respectively. The water content was measured using moisture quick tester (Mettler Toledo MJ33, USA).

2.2.2. Molecular weight (Mw) analysis

The molecular weight of the sample was measured using gel permeation chromatography-eighteen angle laser light scattering instrument (GPC-MALLS). This process was performed using the gel column (Shodex SB-806) and the combined detectors (Wyatt Dawn Heleos II eighteen-angle laser light scattering and Wyatt Optilab rEX refractive index detector). The mobile phase was a 0.1 mol/L sodium chloride solution at a flow rate of 0.5 mL/min, and the column temperature was 40 ℃. The injection volume was 0.1 mL. The sample was dissolved in 0.1 mol/L sodium chloride solution at a concentration of 2 mg/mL.

2.2.3. Monosaccharide composition determination

The polysaccharide sample (10 mg) was hydrolyzed with 4 mol/L trifluoroacetic acid at 120℃ in a sealed tube for 4 h and the hydrolysate was dried with nitrogen to remove excess trifluoroacetic acid. The polysaccharide hydrolysate was dissolved with 10 mL distilled water and then passed through a 0.2 μm microporous filter. Chromatographic separation conditions of fucose (Fuc), rhamnose (Rha), arabinose (Ara), galactose (Gal), glucose (Glc), fructose (Fru), glucuronic acid (GlcA) and galacturonic acid (Gala): Ion Chromatography (IC, DIONEX ICS-3000, USA), CarboPacTMPA10 (4 × 250 mm) analytical column, using sodium acetate (1 mol/L), sodium hydroxide (200 mmol/L) and water as the mobile phase at a flow rate of 1 mL/min. Chromatographic separation conditions of xylose (Xyl) and mannose (Man): IC (DIONEX ICS-3000, USA), CarboPacTMPA20 (3 × 150 mm) analytical column, using sodium hydroxide (250 mmol/L) and water as the mobile phase at a flow rate of 0.5 mL/min. The column temperature was 35 ℃, and 10 μL sample was injected.

2.2.4. Ultraviolet (UV) spectrum scan and Fourier transform infrared spectroscopy (FT-IR)

The spectral data were obtained on a UV-visible spectrophotometer (Metash UV-8000 s, Shanghai, China) at 25 ℃ in the range of 200–600 nm.

The IR spectrum was recorded on a Fourier transform infrared spectroscopy (Bruker Tensor 27, Germany) by grinding a mixture of the sample (2 mg) with dry KBr (100–200 mg for 24 h at 120 ℃) and pressing in a mold. The frequency range was 4000-400 cm^{-1}.

2.2.5. Scanning electron microscope (SEM) analysis

An aliquot of PSP was spread on a mica sheet and sputtered a 20 nm thick gold film under vacuum. Afterwards the surface of the sample was photographed by SEM (Hitachi SU8010, Japan).

2.2.6. Atomic force microscope (AFM) analysis

2.5 μL of 0.2 mg/mL PSP solution was deposited on a clean mica disk and dried at 20 ℃. Then the imagines were observed by AFM (Park NX10, Korea).

 doi:10.20944/preprints202312.2054.v1

2.3. Animal experiment

2.3.1. Evaluation of PSP after acute administration

Firstly, in order to determine the intervention doses of PSP in subsequent experiment, zebrafish were randomly divided into 6 groups: CON (control group), PSP (50 mg/L), PSP (100 mg/L), PSP (200 mg/L), PSP (400 mg/L) and PSP (800 mg/L). Zebrafish were housed in groups of 15 per tank in 10 L tanks. PSP was dissolved in another container with filtered system water. After feeding in the morning, the zebrafish were transferred to the container of PSP with the corresponding concentration and immersed for 1 h, continuously immersing for 9 days. Fish in CON group were not subjected to any administration. The novel tank test (NTT) was performed on day 8 and 9.

2.3.2. CUMS procedure and PSP administration

The CUMS procedure was performed as previously described with appropriate modification (Song et al., 2018). The following stimuli were selected for study: predator exposure, predator water, net chasing, crowding, darkness, light-dark exposure, super-bright light, social isolation, red bucket, tri-colored cups, food deprivation, shallow water exposure, alarm pheromone, air exposure, shaking. Zebrafish were continuously exposed to several unpredictable stressors for 5 weeks. The zebrafish in the control group were separated from the stressed groups. The details of the CUMS protocol were exhibited in Table S1.

The animals were given 14 days to acclimation and then divided into 5 groups: CON (not subjected to any stress), CUMS (CUMS procedure), FLU (FLU 0.1 mg/mL treatment + CUMS), PSP-L (PSP 100 mg/L + CUMS), PSP-H (PSP 200 mg/L + CUMS). Zebrafish were housed in groups of 30 per tank in 10 L tanks. Except for the CON group, the CUMS, FLU, PSP-L and PSP-H group were subjected to CUMS procedure after feeding in the morning for 5 weeks. Start from the 4 th week of CUMS procedure, the zebrafish were transferred to the container of FLU and PSP with the corresponding concentration and immersed for 1 h. FLU and PSP treatment continuously for 9 days (day 29–38) before the beginning of the daily CUMS procedure and behavior tests. Fish in CUMS group were immersed in system water without PSP and fish in CON group were not subjected to any administration. The body weight of zebrafish was monitored (day 35) and NTT and the light and dark tank test (LDT) were performed after the CUMS procedure and administration (day 35–38). The schedule of the animal experiment was exhibited in Figure 2A.

2.4. Behavioral tests

2.4.1. Body weight

The body weight of zebrafish was monitored on day 0 and 35. The weight of the beaker with water was measured. Then zebrafish was fished out with a dry net and quickly put into the measuring beaker, calculating the weight difference before and after. The excess water needs to be drained during the transfer process.

2.4.2. Novel tank test (NTT)

The novel tank test was conducted as previously described (Egan et al., 2009). NTT was performed between 9:00 am and 6:00 pm. All zebrafish fasted for 24 h before NTT. The apparatus was a 2.5 L rectangular tank (25 cm length × 5 cm width × 20 cm height) and maximally filled with water. It was divided into two equal virtual horizontal portions by a line marking the outside walls. A single zebrafish in the tank was recorded for 5 min with a high-definition camera to manually score the latency to top (time taken to cross the line for the first time, s), time spent in top (s), top entries (the number of transitions to top).

 doi:10.20944/preprints202312.2054.v1

2.4.3. Light and dark tank test (LDT)

The light and dark tank test was performed according to a previous report (Cachat et al., 2013). LDT was performed between 9:00 am and 6:00 pm. All zebrafish fasted for 24 h before LDT. The apparatus was a 10 L rectangular tank (28 cm length × 20 cm width × 18 cm height) and maximally filled with water. It was divided into two equal portions: dark and light. A partition could be inserted between the bright and dark areas. The zebrafish could move when removing the partition. A single zebrafish was placed in the dark areas with partition inserted to acclimation for 2 min and recorded for 5 min with a high-definition camera after removing the partition to manually score the time spent in light (s), light entries (the number of transitions to light area).

2.5. Sample collection

All zebrafish were immediately sacrificed in ice water bath after behavior tests. Head and body of zebrafish were separated on the ice. The whole-brain samples were collected for gene expression studies and quickly frozen in liquid nitrogen. Mesencephalic and telencephalic regions were collected in corresponding fixed solutions for further pathological and morphological analyses. The headless whole-body samples of zebrafish were collected and quickly frozen in liquid nitrogen. The whole-brain and whole-body samples were stored at −80°C for further assays.

2.6. Nissl staining

After sacrifice, the mesencephalon samples were paraffin embedded after being fixed with 4% paraformaldehyde. Then, the paraffin sections (4 μm) were dewaxed and rehydrated. The sections were incubated with toluidine blue for 5 min at room temperature. The sections were then differentiated with 0.1% glacial acetic acid for several seconds followed by rinsing in double distilled water and cleared in xylene, and covered by neutral resins and then examined under microscope (Nikon DS-U3, Japan). The integrated optical density (IOD) was counted with Image J software (National Institutes of Health, USA).

2.7. Transmission electron microscope (TEM) observation

After sacrifice, the telencephalon and mesencephalon samples were quickly divided into small pieces on ice and fixed in 2% glutaraldehyde. Post-fixation, samples were immersed in 1% osmium tetraoxide for 2 h at 4 °C and then dehydrated using 50, 70, 90 and 100% alcohol. Samples were embedded in Epon 812 and ultrathin sections (40–50 nm) were contrasted with uranyl acetate followed by lead citrate, and examined with TEM (Hitachi H-7500, Japan) (Chandrasekar et al., 2011).

2.8. Immunohistochemistry

The immunohistochemical analysis was carried out according to the previous study (Togao et al., 2020). Samples of mesencephalon are fixed, embedded, and sectioned in the same manner as Nissl staining. After retrieving the antigen with citrate buffer (pH = 6.0) and quenching endogenous peroxidase activity with 0.3% H_2O_2, the sections were blocked with 3% BSA. Then, the sections were incubated overnight at 4 °C with Iba-1 antibody (ab178847, Abcam) and washed and incubated with secondary antibodies for 1 h at room temperature and stained with DAB. The sections were counterstained, dehydrated, and then examined under microscope (Nikon DS-U3, Japan). The proportion of positive area was counted with Image J software.

2.9. RNA Isolation and Real-Time Quantitative PCR

Three zebrafish whole brains were used to prepare a single sample. RNA was isolated according to the EASYspinPlus rapid tissue/cellular RNA extraction kit (Aidlab Biotechnologies, China). GoScript Reverse Transcription System (Promega Biotech, China) was used for synthesis of cDNA. qRT-PCR was performed in Applied Biosystems QuantStudio 7 Flex system (Thermo FisherScientific, United States) using NovoStart SYBR qPCR SuperMix Plus kit (Novoprotein, China). Relative gene

 doi:10.20944/preprints202312.2054.v1

expression was calculated using the $2^{-\Delta\Delta CT}$ method and normalized with control gene β-actin. Primers information is shown in Table 1.

Table 1. Primer sequences used in real-time quantitative PCR assay.

Gene	Forward Primer	Reverse Primer
β-actin	ACCACGGCCGAAAGAGAAAT	ATGTCCACGTCGCACTTCAT
inos	CCTCCTCATGTACCTGAATCTCG	GCTCCTTGCTTTAGTATGTCGC
cd11b	TCCTCGGATTCCAGAAACAC	AGCAGCACAAGTCCTCCAAT
ym1	GCAAGAGGAAGTCCACCTGAAGAC	ATACAGCAGCGGTCAGCATAAGC
arg-1	TCCGTTCTCCAAAGGACAGC	GACTCGTCGTTGGGAAGGTT
cd206	ACGCTTTCGATGGGTTTCCT	CCCTCCGTAGTACATTCCGC
egr-2	TCTGGATGCGGAGAGGTCTATCAAG	AGTAGGATGGCGGAGGATATGAGATG
il-4	TTGGTCCCCGTTTCTGAGTC	CCAGTCCCGGTATATGCTGC
il-10	AAGCACTCCACAACCCCAAT	TGCATTTCACCATATCCCGCT
il-6	AGACCGCTGCCTGTCTAAAA	TTTGATGTCGTTCACCAGGA
il-1β	TTCCCCAAGTGCTGCTTATT	AAGTTAAAACCGCTGTGGTCA

2.10. Enzyme-linked immunosorbent assay (ELISA)

The headless whole-body samples were used to measure the levels of CORT, TNF-α, IL-1β, IL-6 and IL-10 using commercial ELISA kits (Jianglai Biological Technology, Shanghai, China). Briefly, the headless body sample of single zebrafish was cut into small pieces on ice and homogenized with electric grinder in 1 mL PBS, centrifuged at 10,000 g for 10 min, 4°C. Collecting supernatant and testing based on the manufacturer's instructions.

2.11. Statistical analysis

Software used for the statistical analysis included SPSS 23.0, GraphPad Prism 8.0, and Image J. The results were expressed as mean ± standard error mean (Mean ± SEM). The homogeneity and normality were checked and then One-way ANOVA followed by Fisher's least significant difference (LSD) test was applied to compare the difference among groups. $p < 0.05$ was considered statistically significant.

3. Results

3.1. Structure characterization of PSP

3.1.1. Chemical, molecular weight (Mw) and monosaccharide composition of PSP

As listed in Table 2, PSP sample used in the present study was a crude polysaccharide. It contained 72.12% of total carbohydrates, 14.40% of protein, 5.68% of ash, 3.21% of water, 0.28% of flavonoids, 0.11% of phenols and 0.03% of crude fat, indicating that PSP samples used in this study did not contain other functional active ingredients except for polysaccharide itself, which would not affect the results of subsequent studies on the antidepressant-like effects of PSP.

The molecular weight of the crude PSP determined by GPC/MALLS was 20.48 kDa. The GPC/MALLS profile (Figure 1B) demonstrated that PSP showed an asymmetrical broad peak. The polydispersity Mw/Mn 9.394 (Table 2) also indicated that PSP was a relatively wide distribution sample.

IC analysis (Figure 1D) demonstrated that PSP was composed of Glc, Man, and Gal, with a relative molar ratio of 98.47: 1.07: 0.45. The molar ratio of the three types of monosaccharides indicated that Glc was the major components of PSP.

Preprints (www.preprints.org) | NOT PEER-REVIEWED | Posted: 27 December 2023 doi:10.20944/preprints202312.2054.v1

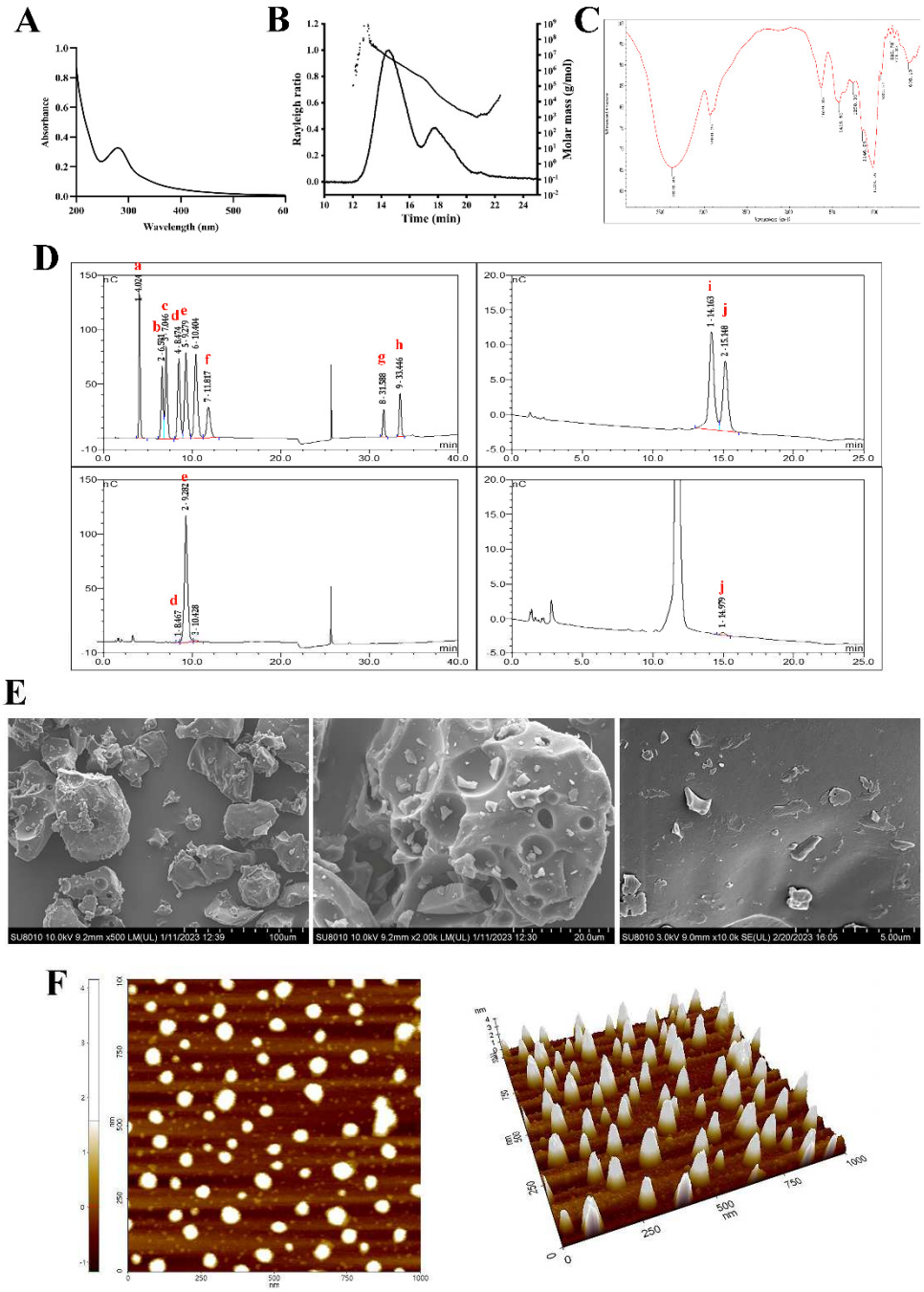

Figure 1. Structure characterization of PSP. (**A**) Ultraviolet spectrum scan, (**B**) Molecular weight, (**C**) Fourier transform infrared spectroscopy, (**D**) Monosaccharide composition, (**E**) Scanning electron microscope and (**F**) Atomic force microscope results of PSP. (a. Fucose; b. Rhamnose; c. Arabinose; d. Galactose; e. Glucose; f. Fructose; g. Glucuronic acid; h. Galacturonic acid; i. Xylose; j. Mannose).

Table 2. The chemical, molecular weight (Mw) and monosaccharide composition of PSP. (Mean ± SEM).

Items	PSP
Molar mass moments (g/mol)	
Mw[a]	$2.048 \times 10^4 \pm 0.03$
Mn[b]	$2.180 \times 10^3 \pm 0.05$
Mp[c]	$1.557 \times 10^3 \pm 0.04$
Mz[d]	$7.340 \times 10^6 \pm 0.08$
Polydispersity	

 doi:10.20944/preprints202312.2054.v1

Mw/Mn	9.394 ± 0.08
Chemical composition (%, w/w)	
Total carbohydrate	72.12 ± 0.90
Protein	14.40 ± 0.004
Ash	5.68 ± 0.51
Water	3.21 ± 0.08
Flavonoids	0.28 ± 0.06
Phenols	0.11 ± 0.003
Crude fat	0.03 ± 0.008

[a] Weight-average molecular weight, [b] Number-average molecular weight, [c] Peak-position molecular weight, [d] Z-average molecular weight.

3.1.2. UV and FT-IR analysis

The weak absorption peak at wavelength 280 nm in the UV spectrum (Figure 1A) confirmed that PSP sample contained protein and might be a glycoprotein, which was in accordance with the protein content. The absence of absorption peak at wavelength 260 nm confirmed that PSP sample was devoid of nucleic acid.

The IR spectrum of PSP is shown in Figure 1C. The sample showed typical absorption peaks of polysaccharides at 3378 cm^{-1} and 2930 cm^{-1}, which were attributed to the O-H and C-H stretching vibration, respectively. The absorption peaks at 1629 cm-1 corresponded to the asymmetric stretching of the carboxylate anions (COO-). The absorption peaks, at approximately 1420 cm^{-1}, were attributed to symmetric stretching of carboxylate anions (COO-) (Zhao et al., 2020). Pyranose ring could account for the 1146 cm^{-1} and 1024 cm^{-1} signals, which were corresponded to the C-O-C stretching vibration and were the typical signal of glucan. The peak at 930 cm^{-1} was ascribed to the presence of β-glucoside bond. The absorption around 822 cm^{-1} and 771 cm^{-1} implied the existence of α-hexapyranose (Zhu et al., 2019). The lack of an absorption peak at 1740 cm^{-1} suggested that PSP did not contain uronic acid (Pei et al., 2015).

3.1.3. Conformational structure analysis of PSP

SEM and AFM method were applied to study the conformational morphological properties of PSP. The SEM images of PSP were shown in Figure 1E. PSP samples showed a tight structure and particles accumulation (×500). The surface texture of PSP was smooth with various-sized holes (×2000). It could be observed clearly that the surface structure was compact and full of snowflake particle when the image was enlarged to ×10000. The polysaccharide's internal voids contribute to its good water-solubility and enable it to engage with cell receptors, which allow it to exhibit more biological functions (Yu et al., 2023).

AFM is a valuable tool for determination of morphological characteristics and molecular parameters of polysaccharides. The AFM planar and 3-dimensional images of the PSP are shown in Figure 1F. PSP exhibited a rough surface, compact and asymmetric shape with the height ranging from -1 to 4 nm, which much higher than that of single chain polysaccharides (generally 0.1–1 nm), indicating that aggregations and inter and intra-molecular interactions occurred in PSP (Yu et al., 2023). The conformation of polysaccharides is closely correlated with their biological activities.

3.2. Effects of PSP on the body weight and depressive-like behaviors of CUMS-induced zebrafish

Firstly, we performed the NTT to determine the intervention doses of PSP in zebrafish. In the NTT, no significant changes in zebrafish behavior were seen in the PSP 50, 100, 200, and 400 mg/L groups. However, the latency to top of the zebrafish in PSP 200 mg/L group showed a decreased tendency and the number of top entries and the time in top showed an increased tendency. The exploratory behavior of zebrafish in the PSP 800 mg/L group was significantly inhibited (Figure 2), with significantly longer latency to top ($p < 0.01$), significantly fewer number to top ($p < 0.01$) and significantly shorter time in top ($p < 0.05$), indicating that higher doses of PSP would have adverse

Preprints (www.preprints.org) | NOT PEER-REVIEWED | Posted: 27 December 2023 doi:10.20944/preprints202312.2054.v1

effects on zebrafish. Based on the behavioral results, PSP 100 and 200 mg/L, which had positive effects on zebrafish behavior and had no toxic side effects, were selected as the intervention doses for subsequent experiments.

As shown in Figure 3E, the initial weight did not significantly differ among groups. After five weeks of CUMS, the weight of zebrafish in the CUMS group was markedly reduced ($p < 0.05$). However, the decreased body weight was improved after FLU (0.1 mg/mL) and PSP (100 and 200 mg/L) treatments ($p < 0.05$).

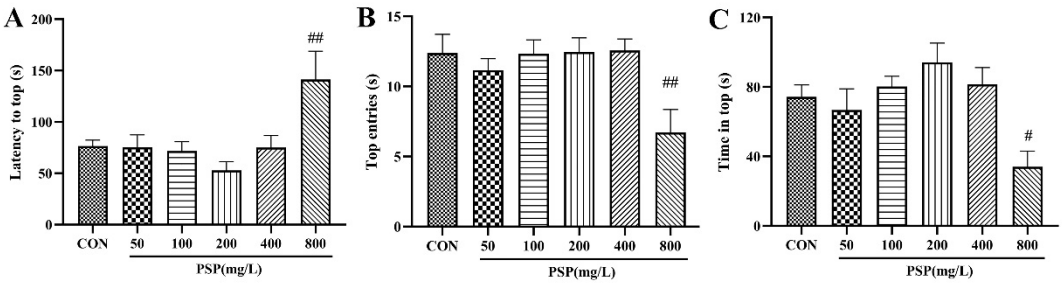

Figure 2. Determination of PSP intervention doses in the novel tank test (NTT). (**A**) Latency to top. (**B**) Top entries. (**C**) Time in top. (n = 12–15). #$p < 0.05$, ##$p < 0.01$ compared with the CON group.

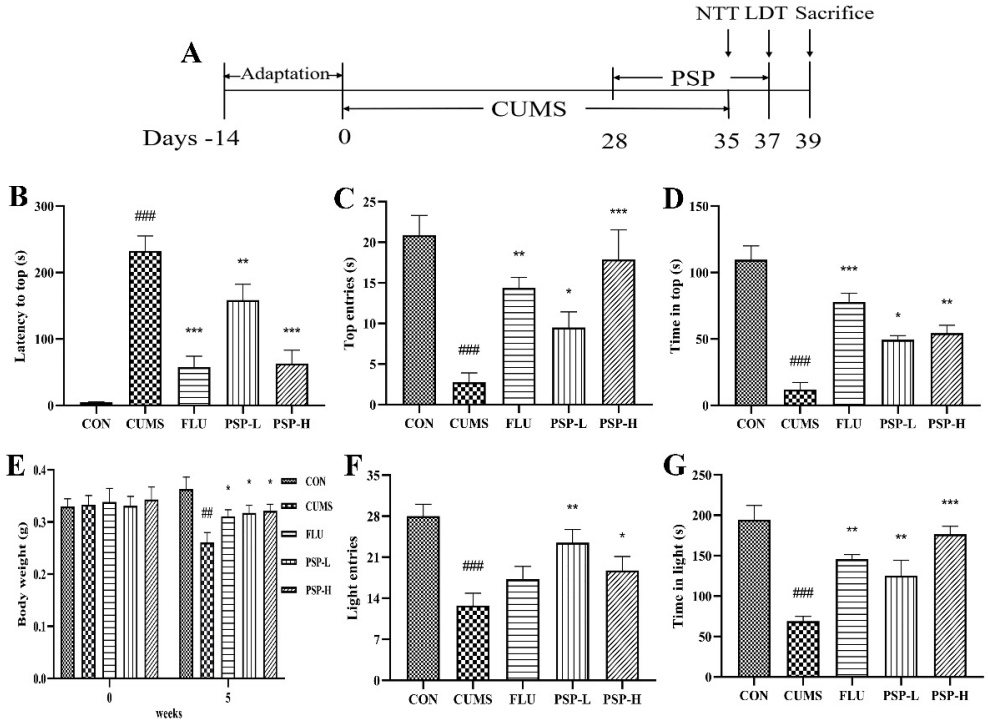

Figure 3. Effects of PSP on the body weight and depressive-like behaviors in CUMS-induced zebrafish. (**A**) Schedule of the experimental procedure. (**B**) Latency to top, (**C**) top entries, and (**D**) time in top in the novel tank test (NTT). (**E**) Changes of the body weight. (**F**) Light entries and (G) time in light in the light and dark tank test (LDT). ($n = 8$). ##$p < 0.01$, ###$p < 0.001$ compared with the CON group, *$p < 0.05$, **$p < 0.01$, ***$p < 0.001$ compared with the CUMS group.

NTT and LDT were both commonly used for evaluating the depressive-like behaviors in zebrafish. Firstly, the CUMS program significantly inhibited the upward exploration behaviors of zebrafish in the NTT, manifested as the increased latency to top (Figure 3B, $p < 0.001$), the reduced number of top entries and the decreased time in top (Figure 3C and D, $p < 0.001$). PSP (100 and 200 mg/L) and FLU (0.1 mg/L) treatment markedly shortened the latency to top (Figure 3B, $p < 0.01$, $p <$

 doi:10.20944/preprints202312.2054.v1

0.001) and increased the number of top entries and the time in top (Figure 3C and D, $p < 0.05$, $p < 0.01$, $p < 0.001$). Then, in the LDT, the CUMS program significantly inhibited the bright area exploration behaviors of zebrafish, manifested as the reduced number of light entries and the decreased time in light area (Figure 3F and G, $p < 0.001$). PSP (100 and 200 mg/L) significantly elevated the number of light entries (Figure 3F, $p < 0.05$, $p < 0.01$). The time in light area markedly increased after PSP (100 and 200 mg/L) and FLU (0.1 mg/L) treatment (Figure 3G, $p < 0.01$, $p < 0.001$). The above results indicated the success of the CUMS model in zebrafish and provided evidence that PSP could significantly ameliorate the depressive-like behaviors in CUMS-induced zebrafish.

3.3. Effects of PSP on the HPI function of CUMS-induced zebrafish

Increased CORT levels suggested hyperactivity of the HPI axis. The results showed that the CORT levels in zebrafish body samples significantly increased after CUMS stimulation (Figure 4A, $p < 0.001$). PSP (100 and 200 mg/L) and FLU (0.1 mg/L) intervention could regulate HPI axis dysfunction because that decreased CORT levels in PSP and FLU groups were observed (Figure 4A, $p < 0.01$).

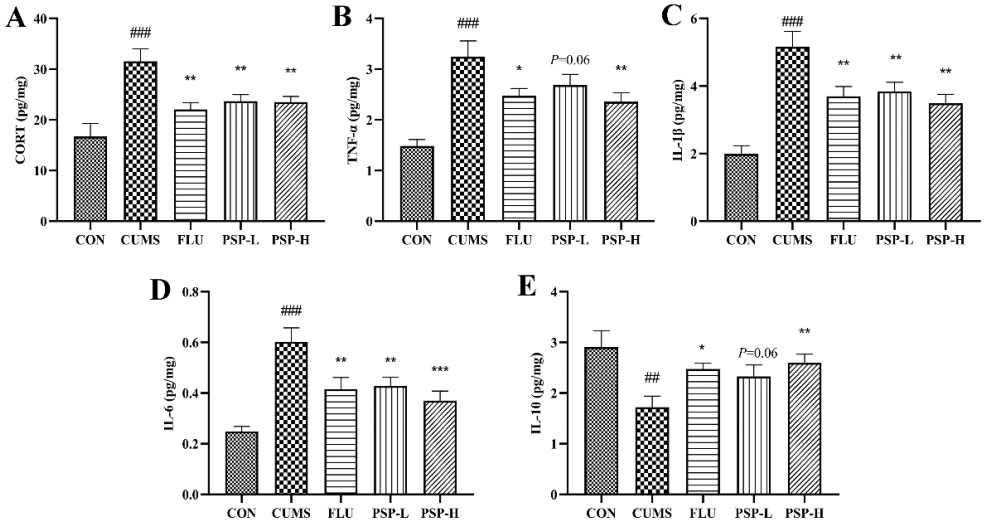

Figure 4. Effects of PSP on the HPI axis and peripheral inflammation in CUMS-induced zebrafish. (**A**) The cortisol (CORT) levels, (**B**) tumor necrosis factor (TNF-α) levels, (**C**) interleukin (IL)-1 levels, (**D**) IL-6 levels and (E) IL-10 levels in body samples. (n = 8). ##$p < 0.01$, ###$p < 0.001$ compared with the CON group, *$p < 0.05$, **$p < 0.01$, ***$p < 0.001$ compared with the CUMS group.

3.4. Effects of PSP on the peripheral inflammation of CUMS-induced zebrafish

The TNF-α, IL-6 and IL-1β levels elevated and the IL-10 levels decreased in the body samples after CUMS exposure (Figure 4B-E, $p < 0.01$, $p < 0.001$). However, the TNF-α levels were significantly reduced by PSP (200 mg/L) and FLU (0.1 mg/L) administration (Figure 4B, $p < 0.05$, $p < 0.01$) and the IL-6 and IL-1β levels were markedly reduced by PSP (100 and 200 mg/L) and FLU (0.1 mg/L) intervention (Figure 4C and D, $p < 0.01$, $p < 0.001$). Administration with PSP (200 mg/L) and FLU (0.1 mg/L) significantly increased the levels of IL-10 (Figure 4E, $p < 0.05$, $p < 0.01$). These results suggested that PSP could suppressing peripheral inflammation.

3.5. Effects of PSP on brain health in CUMS-induced zebrafish

Nissl staining was conducted for exploring the effects of PSP on neuronal damage in the mesencephalon of CUMS-induced zebrafish. As shown in Figure 5A, neurons were regularly arrayed and Nissl bodies were clear in the CON group. Contrast, Nissl bodies disintegration, irregular and sparsely neuronal arrangement were clearly observed in CUMS-induced zebrafish and the IOD value was significantly reduced ($p < 0.001$). The decrease in Nissl-positive neurons and IOD value was significantly reversed after PSP and FLU administrations ($p < 0.001$).

 doi:10.20944/preprints202312.2054.v1

Structure of neurons of zebrafish mesencephalon and telencephalon were observed using TEM (Figure 5B and C). Significant perinuclear gap expansion was observed in both mesencephalon and telencephalon of zebrafish after CUMS exposure. Mitochondrial structure changed obviously after CUMS exposure especially in mesencephalon, including mitochondrial swelling and loss of mitochondrial cristae in neurons. Neuronal damage in the mesencephalon was more severe than that in the telencephalon region. Furthermore, the ultrastructure of blood-brain barrier in telencephalon was observed using TEM (Figure 6). CUMS exposure induced significant basement membrane shrinkage, disrupting the integrity of the BBB. Compared with the CUMS group, PSP and FLU treatments alleviated these pathological changes.

Altogether, these findings implied that PSP could attenuate neuronal and BBB damage induced by CUMS-induced depression in zebrafish.

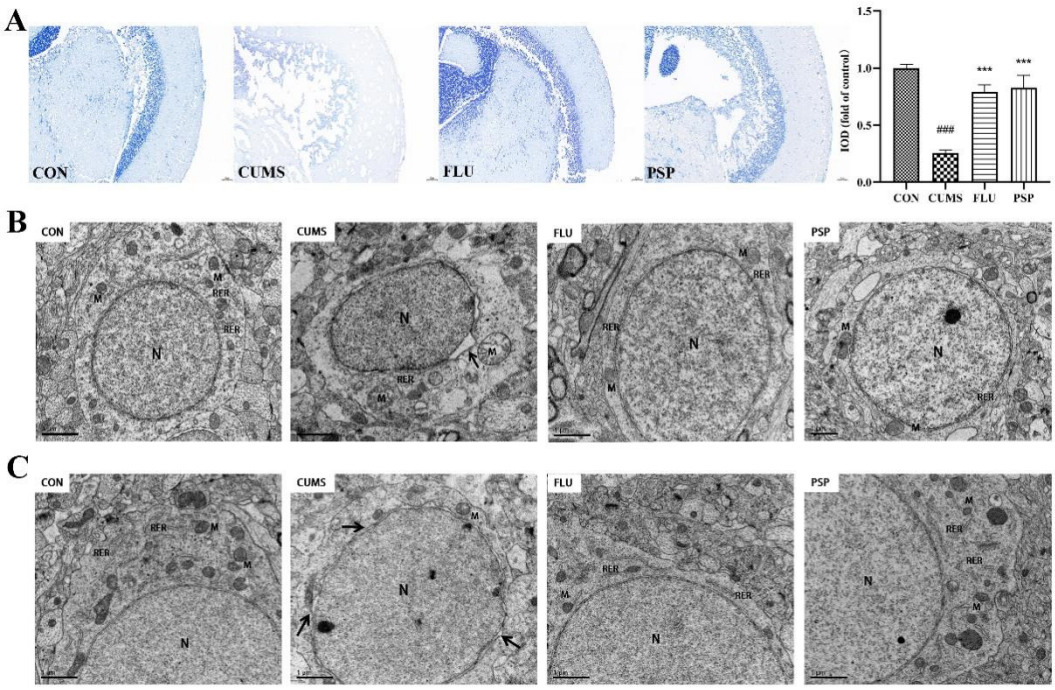

Figure 5. Results of Nissl staining and neuronal ultrastructure of zebrafish in each group. (**A**) Representative Nissl staining images of zebrafish mesencephalon in the CON, CUMS, FLU, and PSP-H group. Neuronal ultrastructure of zebrafish (**B**) mesencephalon and (**C**) telencephalon in the CON, CUMS, FLU, and PSP-H group. (N, the nucleus, M, mitochondria, RER, rough endoplasmic reticulum). ###$p < 0.001$ compared with the CON group, ***$p < 0.001$ compared with the CUMS group.

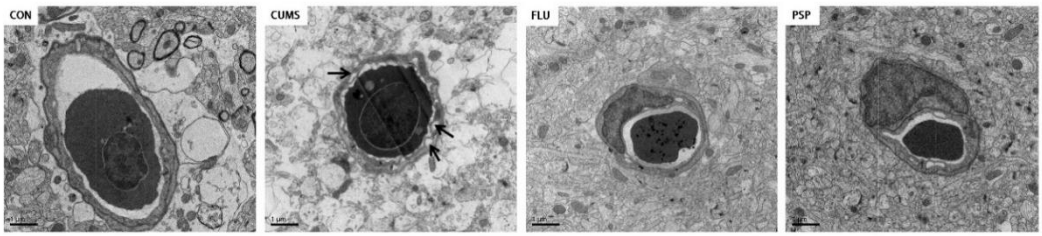

Figure 6. Blood-brain barrier ultrastructure of zebrafish telencephalon in the CON, CUMS, FLU, and PSP-H group.

3.6. Effects of PSP on microglia of CUMS-induced zebrafish

Iba-1 is a marker protein of microglia. Its expression was analyzed by immunohistochemistry to evaluate the activation of microglia. Immunohistochemical (Figure 7) results indicated that the

 doi:10.20944/preprints202312.2054.v1

proportion of positive area in mesencephalon of CUMS-induced zebrafish was markedly higher than the CON group ($p < 0.001$), indicating that microglia was activated after CUMS exposure. The activation of microglia was inhibited by PSP and FLU with significantly reduced proportion of positive area ($p < 0.001$).

Then, to evaluate the effect of PSP on the state transition of microglia, we measured the expression of M1/M2 phenotype markers in the brain of zebrafish. As shown in Figure 8A-J, CUMS significantly increased the expression of M1 phenotype genes (*il-6*, *il-1β*, *inos* and *cd11b*) and decreased the expression of M2 phenotype genes (*cd206* and *ym1*). The mRNA expression of M2 phenotype genes in the CUMS group (*il-4*, *il-10*, *arg-1* and *egr-2*) showed a decreased tendency but no significant changes. These results implied that CUMS stimulation could induce phenotypic changes of microglia. However, when the zebrafish treated with PSP, these changes were notably reversed compared to the CUMS group. PSP significantly decreased CUMS induced up-regulation of M1 phenotype genes expression (*il-6*, *il-1β*, *inos* and *cd11b*), while significantly increased CUMS induced down-regulation of M2 phenotype genes expression (*il-4*, *il-10*, *cd206*, *egr-2* and *ym1*). The expression of *arg-1* was increased but not show significant differences. The above results indicated that PSP could suppress neuroinflammation and modulate microglia M1/M2 polarization to exert the antidepressant-like effects.

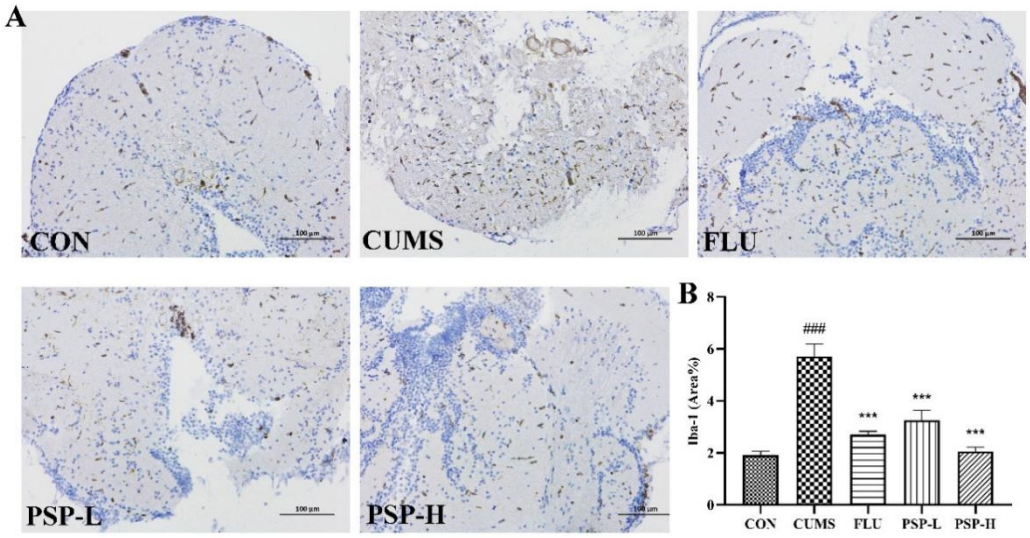

Figure 7. Effects of PSP on the expression of Iba-1 in CUMS-induced zebrafish. (**A**) Representative immunohistochemical images of Iba-1 in the CON, CUMS, FLU, PSP-L and PSP-H group. (**B**) Results of the proportion of Iba-1 positive areas. ($n = 4$). ###$p < 0.001$ compared with the CON group, ***$p < 0.001$ compared with the CUMS group.

Preprints (www.preprints.org) | NOT PEER-REVIEWED | Posted: 27 December 2023 doi:10.20944/preprints202312.2054.v1

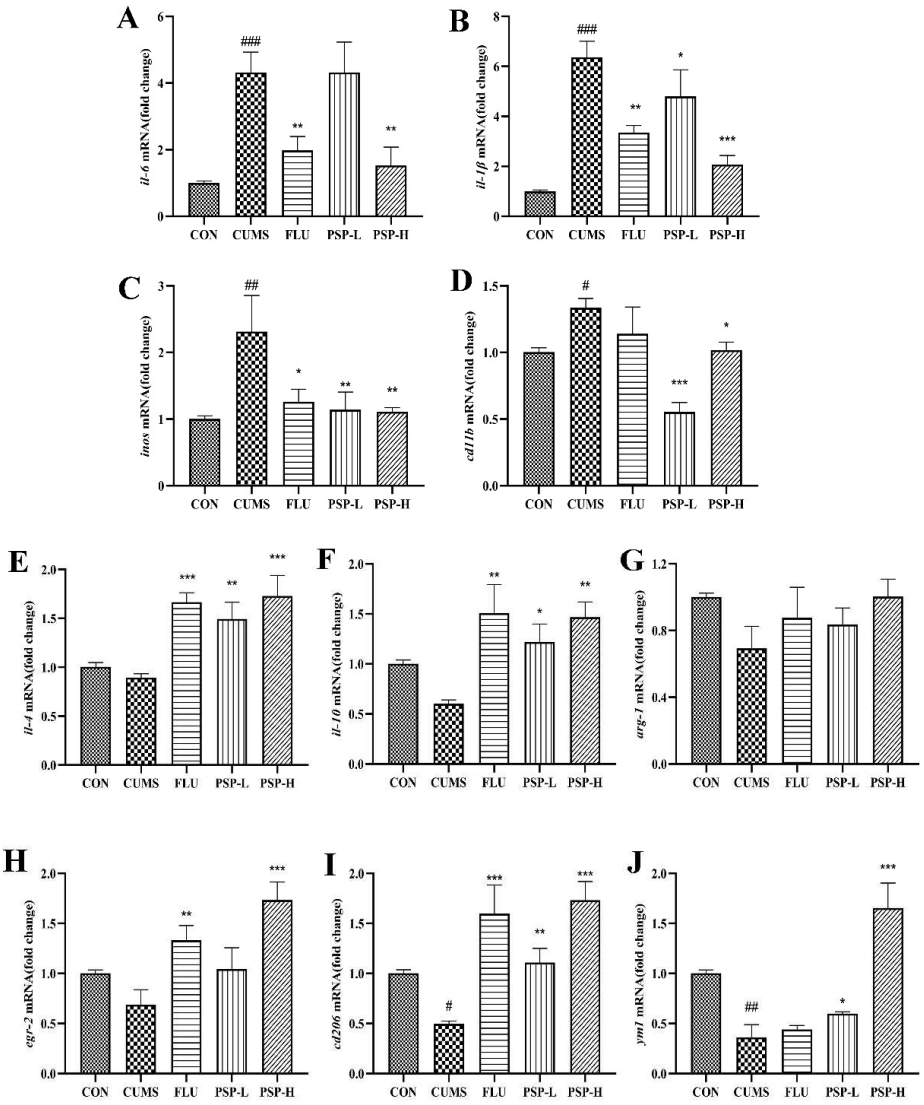

Figure 8. Effects of PSP on mRNA levels of M1/M2 microglial markers in CUMS-induced zebrafish. The mRNA expression of (**A**) il-6, (**B**) il-1 , (**C**) inos, (**D**) cd11b, (**E**) il-4, (**F**) il-10, (**G**) arg-1, (**H**) egr-2, (**I**) cd206 and (**J**) ym1. (n = 6). #p < 0.05, ##p < 0.01, ###p < 0.001 compared with the CON group, *p < 0.05, **p < 0.01, ***p < 0.001 compared with the CUMS group.

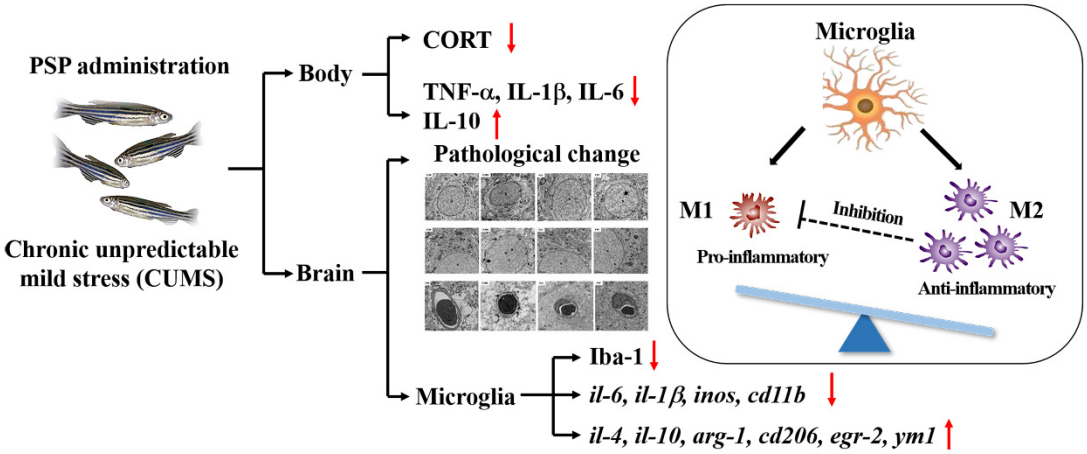

Figure 9. The mechanisms by which PSP exerts antidepressant-like effects in CUMS-induced zebrafish.

 doi:10.20944/preprints202312.2054.v1

4. Discussion

CUMS was initially a procedure designed for rats to mimic the physiological symptoms of clinical depression, which now has become widely accepted as a classic depression model (Willner et al., 1992). In rodent CUMS models, a series of unpredictable mild stimuli are often used, such as food and water deprivation, forced swimming, restraint stress, soiled cage, overnight illumination and so on (D'Aquila et al., 1994). Then the body weight, locomotor activities and the classic behavioral paradigms were performed to evaluate the fundamental state of mice, exploration abilities and depressive-like behaviors (Dang et al., 2022). Behavioral, endocrine, immunological and neuromorphic changes will be observed in the model animals (Guo et al., 2023; Liu et al., 2023). Referring to the rodent CUMS model, the researchers successfully establish a similar depression model in zebrafish using chronic and unpredictable stress, which can also induce strong behavioral and physiological changes in zebrafish. The main stressors currently used on zebrafish are predator exposure, light-dark exposure, net chasing, crowding, shallow water exposure, social isolation, alarm pheromone, air exposure, tri-colored cups (Song, et al., 2018). Several behavioral tests have been developed to assess depression in zebrafish, among which the NTT and LDT are widely used. The NTT can evaluate the depressive-like behavior of zebrafish from the overall movement, upward exploration and freezing. Zebrafish have a preference for darkness, in the LDT, the decreased time in the light area corresponded to the enhancement of anxiety and depression (Fontana et al., 2022). In addition, consistent with rodents, CUMS-induced zebrafish also experiences malnutrition and weight loss (Bensi et al., 1997).

In the present study, the intervention doses of PSP were first determined through the NTT. PSP intervention has a positive impact on zebrafish behavior within a certain dose range. However, excessive intervention doses actually inhibit zebrafish exploratory behavior. We speculate that excessive doses of PSP are toxic to zebrafish. Therefore, PSP (100 and 200 mg/L), which had positive effects on zebrafish behavior and had no toxic side effects, were selected as the intervention concentrations for the subsequent experiments. The body weight of zebrafish was significantly reduced after five weeks of CUMS procedure. The exploratory behaviors of CUMS-induced zebrafish in NTT and LDT were significantly inhibited, demonstrating the success of the CUMS-induced depression model in zebrafish. A significant reversal of these behavioral changes was observed in CUMS-induced zebrafish after administering PSP. The notable antidepressant-like effects of PSP were consistent with the previous studies in mice (Zhang, et al., 2023).

Depression patients not only exhibit behavioral and emotional disorders, but also accompanied by changes in brain structure and dysfunction. In CUMS model of the rodents, neuronal damage characterized by brain tissue atrophy, neuron loss and apoptosis can also be observed (Zeng et al., 2022). The present study evaluated the effects of CUMS and PSP on zebrafish brain neurons through Nissl staining and TEM observation. Nissl staining can reflect the survival of neurons and the level of neuroplasticity to a certain extent. The results showed that neurons were irregularly distributed as well as Nissl bodied disintegrated and the IDO value significantly decreased in the mesencephalon of CUMS-induced zebrafish, which indicated that the neurons are obviously damaged after CUMS exposure. TEM is used to observe the ultrastructure of neurons. Significant perinuclear gap expansion in both mesencephalon and telencephalon and mitochondrial structure damage in mesencephalon were observed of zebrafish after CUMS exposure. PSP significantly alleviated neuronal damage in zebrafish with the increased Nissl bodies, reduced perinuclear expansion and restored mitochondrial structure. BBB is a crucial structure to maintain the proper function of the brain. Disruption of the BBB is observed in several different neurological disorders including depression. Research showed that targeted disruption of the female BBB induced anxiety and depression-like behaviors (Dion-Albert et al., 2022). Recent studies implicate the inflammation may be one of the mechanisms of BBB disruption (Medina-Rodriguez & Beurel, 2022). In this study, PSP partially reversed the BBB disruption, which may be related to its anti-inflammatory effects, and further research is needed afterwards.

The HPA axis can effectively regulate the physiological response to stress, and HPA axis hyperfunction is a typical feature of depression patients and depression model animals. In CUMS

 doi:10.20944/preprints202312.2054.v1

model of the rodents, high level of glucocorticoid produces a range of neurotoxic effects in the prefrontal cortex and hippocampus, inducing microglia activation, neuronal apoptosis, neuroplasticity injury, peripheral and neuroinflammation (Kandola et al., 2019). The HPI axis of zebrafish is structurally and functionally homologous to the HPA axis of mammals. The HPI axis, as the pressure regulation system of fish, plays an important role in maintaining stable status of fish under a variety of physiological or environmental pressures (Wang et al., 2020). In zebrafish, cortisol is the major product of the HPI axis so it is often used as a stress response indicator (Wang et al., 2020). When faced with CUMS stimulation, the CORT levels in the body of zebrafish significantly increased. However, in the present study, it was reversed after PSP and FLU treatment, which was in agreement with the previous studies in mice, suggesting that adjustment of HPA axis might be one of the mechanisms of PSP antidepressant effects (Shen et al., 2022). The functional study of the HPI axis in fish also involves some important receptors, such as glucocorticoid receptor (GR) and mineralocorticoid receptor (MR) (Bury & Sturm, 2007; Schaaf et al., 2009). Further research is needed on the effects of CUMS and PSP on the related receptors and their role in the antidepressant effects.

The bidirectional communication between the endocrine system and the immune system jointly regulates the body's homeostasis. It is known that many cytokines interact with the HPA axis and positively correlated with the degree of depression. TNF-α, IL-1β, and IL-6 are considered to be the major participants in this bidirectional communication (Engelsma et al., 2002). In addition, IL-10 is an important anti-inflammatory cytokine that can inhibit neuronal apoptosis and exert neuroprotective effects by activating the JAK1/STAT3 signaling pathway (Ouyang et al., 2011). IL-10 can also inhibit the activation of microglia and the production of proinflammatory factors (Porro et al., 2020). In our present study, CUMS exposure induced peripheral inflammatory response in zebrafish. The levels of pro-inflammatory cytokines were significantly increased and the release of the anti-inflammatory cytokines was decreased in the body of zebrafish. In contrast, these changes were reversed after PSP administration. PSP could inhibit peripheral inflammation by regulating the balance of pro-inflammatory and anti-inflammatory factors and inhibiting the excessive activation of HPI axis.

Peripheral inflammation and chronic stress can cause neuroinflammation, which is related to activated microglia. Microglia is a multifunctional immune cell in the CNS. It monitors and maintains homeostasis of the internal environment through its own dynamic process (Nimmerjahn et al., 2005). The transformation of microglia from resting ramified state to ameboid active state and functional phenotypes are the focus of attention in neuropsychiatric diseases (Calcia et al., 2016). Inhibiting the over activation and regulating the polarization phenotype of microglia can be potential targets for the treatment of neuropsychiatric disorders. Different polarized phenotypes of microglia, commonly referred to as M1/M2 phenotypes, play destructive and protective roles in the CNS, respectively. M1 phenotype microglia release neurotoxic substances and inflammatory factors leading to neurological dysfunction and inducing inflammatory storm, while M2 phenotype microglia restore CNS homeostasis by blocking inflammatory processes and promoting neurotrophic factor production (Wang et al., 2022). In LPS and CUMS induced depression models of rodents, neuroinflammation accompanied by the increase of M1 microglia and the decrease of M2 microglia was observed (Wang et al., 2022). Zebrafish microglia share a highly conserved signature genes program with their mammalian counterparts. Both also share functional similarities, including responding to danger signals, clearing apoptotic neurons, and fine-tuning neuronal activity (Wu et al., 2020). The activation of microglia also exists in zebrafish. Microglia was activated in Tilapia Lake Virus-infected larvae. The cell shape changed from ramified state to ameboid active state. Strong neuroinflammation was also induced by Tilapia Lake Virus in adult fish and the expression of microglia genes were upregulated (Mojzesz et al., 2021). Administration of IGF-1 morpholino at the lesion site of spinal-transected zebrafish increased the immunofluorescence density of iba-1, suggesting that microglia were activated (Zhao et al., 2022). In the previous study, two distinct microglial subtypes, phagocytotic microglia and regulatory microglia, which may have complementary functions under physiological and pathological conditions, were identified in adult zebrafish. Phagocytotic microglia are amoeboid in shape but regulatory microglia have ramified protrusions. The former is highly

mobile and phagocytotic while the latter is the opposite (Wu, et al., 2020). In this study, the activation status and polarization phenotypes of microglia and neuroinflammation in CUMS-induced zebrafish were investigated with reference to rodent microglia marker genes. Our results suggested that CUMS exposure in zebrafish induced neuroinflammation, microglia activation and promoted M1 phenotype polarization. PSP was important modulator of microglial inflammation by inhibiting microglia activation and promoting M2 phenotype polarization. It is of great significance to understand the role of microglia in depression and the regulation of PSP on microglia.

The efficacy of polysaccharide is closely related to its structure, including molecular weight, composition of monosaccharide, type of glycosidic bond, chemical modification, etc. Studying the structure-activity relationship of polysaccharides is of great significance for in-depth research on biological activity and its development and utilization. Most polysaccharides having antidepressant-like effects are heteropolysaccharides composed of two or more monosaccharides with a high proportion of Glc. Those containing a β-glycosidic bond appear to have good antidepressant activity (Guo et al., 2023). The structure of PSP in this study conforms to the above rules. However, there is currently limited research on the relationship between the structure and antidepressant effects of polysaccharides, and further research is needed in the future.

5. Conclusion

In the current study, PSP samples had the typical structure characteristics of polysaccharide, consisting of Glc, Man, and Gal with the average Mw 20.48 kDa. Conformational structure results showed that PSP owned a porous and agglomerated morphology. Besides, PSP effectively reversed the depressive-like behaviors in CUMS-induced depression model in zebrafish. Its antidepressant-like effects might be mediated by altering the HPI axis dysfunction, suppressing peripheral inflammation, inhibiting neuroinflammation induced by microglia hyperactivation, and modulating microglial M1/M2 polarization. These findings provide a new insight into the potential of PSP used in exploitation for the functional foods of emotional regulation.

Author Contributions: C. L. and F. Z. W. designed the study. Y. Y. Z. conducted the experiments and collected the data. D. Y. W., J. M. L.,B. F., and Y. J. B. helped with data analysis. Y. Y. Z. wrote this paper. C. L., and F. Z. W. revised the manuscript. All authors approved the final manuscript.

Funding: This work was supported by National Key Research and Development Program of China (No.2023YFD2201300), Chinese Academy of Agricultural Sciences (CAAS-ASTIP-2023-IFST) and China Agriculture Research System (CARS-04-PS29).

Data Availability Statement: The data that support the findings of this study are available from the corresponding author upon reasonable request.

Conflicts of Interest: The authors declare that they have no known competing financial interests or personal relationships that could have appeared to influence the work reported in this paper.

Abbreviations

BBB, blood-brain barrier; CNS, central nervous system; CORT, cortisol; CUMS, chronic unpredictable mild stress; ELISA, enzyme-linked immunosorbent assay; FLU, fluoxetine hydrochloride; HPA, hypothalamic-pituitary-adrenal axis; HPI, hypothalamic-pituitary-interrenal axis; IOD, the integrated optical density; LDT, light and dark tank test; NTT, novel tank test; PSP, Polygonum sibiricum polysaccharide; TNF-α, tumor necrosis factor; IL-1β, interleukin-1β; IL-6, interleukin-6; IL-10, interleukin-10.

References

1. Bao, Y. F., Li, J. Y., Zheng, L. F., & Li, H. Y. 2015. Antioxidant activities of cold-nature Tibetan herbs are signifcantly greater than hot-nature ones and are associated with their levels of total phenolic components. Chin J Nat Medicines. 13 (8), 609-617. https://doi.org/10.1016/S1875-5364(15)30057-1

2. Bensi, N., Bertuzzi, M., Armario, A., & Gauna, H. F. 1997. Chronic immobilization stress reduces sodium intake and renal excretion in rats. Physiol Behav. 62 (6), 1391-1396. https://doi.org/10.1016/s0031-9384(97)00197-2
3. Bury, N. R., & Sturm, A. 2007. Evolution of the corticosteroid receptor signalling pathway in fish. Gen Comp Endocr. 153 (1-3), 47-56. https://doi.org/10.1016/j.ygcen.2007.03.009
4. Cachat, J., Kyzar, E. J., Collins, C., Gaikwad, S., Green, J., Roth, A., El-Ounsi, M., Davis, A., Pham, M., Landsman, S., Stewart, A. M., & Kalueff, A. V. 2013. Unique and potent effects of acute ibogaine on zebrafish: the developing utility of novel aquatic models for hallucinogenic drug research. Behav Brain Res. 236 (1), 258-269. https://doi.org/10.1016/j.bbr.2012.08.041
5. Calcia, M. A., Bonsall, D. R., Bloomfield, P. S., Selvaraj, S., Barichello, T., & Howes, O. D. 2016. Stress and neuroinflammation: a systematic review of the effects of stress on microglia and the implications for mental illness. Psychopharmacology. 233 (9), 1637-1650. https://doi.org/10.1007/s00213-016-4218-9
6. Cao, L. H., Zhao, Y. Y., Bai, M., Geliebter, D., Geliebter, J., Tiwari, R., He, H. J., Wang, Z. Z., Jia, X. Y., Li, J., Li, X. M., & Miao, M. S. 2022. Mechanistic studies of Gypenosides in microglial state transition and its implications in depression-like behaviors: role of TLR4/MyD88/NF-kappaB signaling. Front Pharmacol. 13, 838261. https://doi.org/10.3389/fphar.2022.838261
7. Chandrasekar, G., Arner, A., Kitambi, S. S., Dahlman-Wright, K., & Lendahl, M. A. 2011. Developmental toxicity of the environmental pollutant 4-nonylphenol in zebrafish. Neurotoxicol Teratol. 33 (6), 752-764. https://doi.org/10.1016/j.ntt.2011.09.009
8. Dang, R. Z., Wang, M. Y., Li, X. H., Wang, H. Y., Liu, L. X., Wu, Q. Y., Zhao, J. T., Ji, P., Zhong, L. M., Licinio, J., & Xie, P. 2022. Edaravone ameliorates depressive and anxiety-like behaviors via Sirt1/Nrf2/HO-1/Gpx4 pathway. J Neuroinflamm. 19 (1), 41. https://doi.org/10.1186/s12974-022-02400-6
9. D'Aquila, P. S., Brain, P., & Willner, P. 1994. Effects of chronic mild stress on performance in behavioural tests relevant to anxiety and depression. Physiol Behav. 56 (5), 861-867. https://doi.org/10.1016/0031-9384(94)90316-6
10. Deng, J. W., Zhou, F. W., Hou, W. T., Silver, Z., Wong, C., Y., Chang, O., Huang, E. & Zuo, K., Q. 2021. The prevalence of depression, anxiety, and sleep disturbances in COVID-19 patients: a meta-analysis. Ann NY Acad Sci. 1486 (1), 90-111. https://doi.org/10.1111/nyas.14506
11. Dion-Albert, L., Cadoret, A., Doney, E., Kaufmann, F. N., Dudek, K. A., Daigle, B., Parise, L. F., Cathomas, F., Samba, N., Hudson, N., Lebel, M., Signature, C., Campbell, M., Turecki, G., Mechawar, N., & Menard, C. 2022. Vascular and blood-brain barrier-related changes underlie stress responses and resilience in female mice and depression in human tissue. Nat Commun. 13 (1), 164. https://doi.org/10.1038/s41467-021-27604-x
12. DuBois, M., Gilles, K. A., Hamilton, J. K., Rebers, P. A., & Smith, F. 1956. Colorimetric method for determination of sugars and related substances. Anal Chem. 28 (3), 350-356. https://doi.org/10.1021/ac60111a017
13. Egan, R. J., Bergner, C. L., Hart, P. C., Cachat, J. M., Canavello, P. R., Elegante, M. F., Elkhayat, S. I., Bartels, B. K., Tien, A. K., Tien, D. H., Mohnot, S., Beeson, E., Glasgow, E., Amri, H., Zukowska, Z., & Kalueff, A. V. 2009. Understanding behavioral and physiological phenotypes of stress and anxiety in zebrafish. Behav Brain Res, 205 (1), 38-44. https://doi.org/10.1016/j.bbr.2009.06.022
14. Engelsma, M. Y., Huising, M. O., van Muiswinkel, W. B., Flik, G., Kwang, J., Savelkoul, H. F., & Verburg-van Kemenade, B. M. 2002. Neuroendocrine-immune interactions in fish: a role for interleukin-1. Vet Immunol Immunop, 87 (3-4), 467-479. https://doi.org/10.1016/s0165-2427(02)00077-6
15. Fontana, B. D., Alnassar, N., & Parker, M. O. 2022. The zebrafish (Danio rerio) anxiety test battery: comparison of behavioral responses in the novel tank diving and light-dark tasks following exposure to anxiogenic and anxiolytic compounds. Psychopharmacology. 239 (1), 287-296. https://doi.org/10.1007/s00213-021-05990-w
16. Gao, C., Xu, J., Liu, Y., & Yang, Y. X. 2021. Nutrition policy and healthy China 2030 building. Eur J Clin Nutr. 75 (2), 238-246. https://doi.org/10.1038/s41430-020-00765-6
17. Guo, S. R., Wang, H., & Yin, Y. F. 2022. Microglia polarization from M1 to M2 in neurodegenerative diseases. Front Aging Neurosci. 14, 815347. https://doi.org/10.3389/fnagi.2022.815347
18. Guo, Y. X., Chen, X. F., Cong, P., Li, Z. X., Wu, Y. P., Zhang, J., Wang, J. T., Yao, W. B., Yang, W. J., & Chen, F. X. 2023. Advances in the mechanisms of polysaccharides in alleviating depression and its complications. Phytomedicine. 109, 154566. https://doi.org/10.1016/j.phymed.2022.154566

19. Kandola, A., Ashdown-Franks, G., Hendrikse, J., Sabiston, C. M., & Stubbs, B. 2019. Physical activity and depression: towards understanding the antidepressant mechanisms of physical activity. Neurosci Biobehav R. 107, 525-539. https://doi.org/10.1016/j.neubiorev.2019.09.040
20. Liu, E. Y., Yang, C. L., Tsai, J. C., Cheng, H. Y., & Peng, W. H. 2023. Antidepressive mechanisms of rhynchophylline in mice with chronic unpredictable stress-induced depression. J Ethnopharmacol. 309, 116302. https://doi.org/10.1016/j.jep.2023.116302
21. Medina-Rodriguez, E. M., & Beurel, E. 2022. Blood brain barrier and inflammation in depression. Neurobiol Dis. 175, 105926. https://doi.org/10.1016/j.nbd.2022.105926
22. Mojzesz, M., Widziolek, M., Adamek, M., Orzechowska, U., Podlasz, P., Prajsnar, T. K., Pooranachandran, N., Pecio, A., Michalik, A., Surachetpong, W., Chadzinska, M., & Rakus, K. 2021. Tilapia lake virus-induced neuroinflammation in zebrafish: microglia activation and sickness behavior. Front Immunol. 12, 760882. https://doi.org/10.3389/fimmu.2021.760882
23. Moret, C., Isaac, M., & Briley, M. 2009. Problems associated with long-term treatment with selective serotonin reuptake inhibitors. J Psychopharmacol. 23 (8), 967-974. https://doi.org/10.1177/0269881108093582
24. Nimmerjahn, A., Kirchhoff, F., & Helmchen, F. 2005. Resting microglial cells are highly dynamic surveillants of brain parenchyma in vivo. Science. 308 (5726), 1314-1318. https://doi.org/10.1126/science.1110647
25. Ouyang, W., Rutz, S., Crellin, N. K., Valdez, P. A., & Hymowitz, S. G. 2011. Regulation and functions of the IL-10 family of cytokines in inflammation and disease. Annu Rev Immunol. 29, 71-109. https://doi.org/10.1146/annurev-immunol-031210-101312
26. Pei, J. J., Wang, Z. B., Ma, H. L., & Yan, J. K. 2015. Structural features and antitumor activity of a novel polysaccharide from alkaline extract of Phellinus linteus mycelia. Carbohyd Polym. 115, 472-477. https://doi.org/10.1016/j.carbpol.2014.09.017
27. Porro, C., Cianciulli, A., & Panaro, M. A. 2020. The regulatory role of IL-10 in neurodegenerative diseases. Biomolecules. 10 (7). https://doi.org/10.3390/biom10071017
28. Schaaf, M. J., Chatzopoulou, A., & Spaink, H. P. 2009. The zebrafish as a model system for glucocorticoid receptor research. Comp Biochem Phys A. 153 (1), 75-82. https://doi.org/10.1016/j.cbpa.2008.12.014
29. Shen, F. M., Song, Z. J., Xie, P., Li, L., Wang, B., Peng, D. Y., & Zhu, G. Q. 2021. Polygonatum sibiricum polysaccharide prevents depression-like behaviors by reducing oxidative stress, inflammation, and cellular and synaptic damage. J Ethnopharmacol. 275, 114164. https://doi.org/10.1016/j.jep.2021.114164
30. Shen, F. M., Xie, P., Li, C. T., Bian, Z. J., Wang, X. C., Peng, D. Y., & Zhu, G. Q. 2022. Polysaccharides from Polygonatum cyrtonema Hua reduce depression-like behavior in mice by inhibiting oxidative stress-calpain-1-NLRP3 signaling axis. Oxid Med Cell Longev. 2022, 2566917. https://doi.org/10.1155/2022/2566917
31. Song, C., Liu, B. P., Zhang, Y. P., Peng, Z., Wang, J., Collier, A. D., Echevarria, D. J., Savelieva, K. V., Lawrence, R. F., Rex, C. S., Meshalkina, D. A., & Kalueff, A. V. 2018. Modeling consequences of prolonged strong unpredictable stress in zebrafish: Complex effects on behavior and physiology. Prog Neuro-Psychoph. 81, 384-394. https://doi.org/10.1016/j.pnpbp.2017.08.021
32. Togao, M., Nakayama, S. M. M., Ikenaka, Y., Mizukawa, H., Makino, Y., Kubota, A., Matsukawa, T., Yokoyama, K., Hirata, T., & Ishizuka, M. 2020. Bioimaging of Pb and STIM1 in mice liver, kidney and brain using laser ablation inductively coupled plasma mass spectrometry (LA-ICP-MS) and immunohistochemistry. Chemosphere. 238, 124581. https://doi.org/10.1016/j.chemosphere.2019.124581
33. Vegh, R., Csoka, M., Stefanovits-Banyai, E., Juhasz, R., & Sipos, L. 2022. Biscuits enriched with monofloral bee pollens: Nutritional properties, techno-functional parameters, sensory profile, and consumer preference. Foods. 12 (1), 18. https://doi.org/10.3390/foods12010018
34. Walker, J. M. 1994. The bicinchoninic acid (BCA) assay for protein quantitation. Methods in molecular biology. 32, 5-8. https://doi.org/10.1385/0-89603-268-X:5
35. Wang, H. X., He, Y., Sun, Z. L., Ren, S. Y., Liu, M. X., Wang, G., & Yang, J. 2022. Microglia in depression: an overview of microglia in the pathogenesis and treatment of depression. J Neuroinflamm. 19 (1), 132. https://doi.org/10.1186/s12974-022-02492-0
36. Wang, L., Li, M., Zhu, C. P., Qin, A. P., Wang, J. C., & Wei, X. N. 2022. The protective effect of Palmatine on depressive like behavior by modulating microglia polarization in LPS-induced mice. Neurochem Res. 47 (10), 3178-3191. https://doi.org/10.1007/s11064-022-03672-3

37. Wang, L. K., Lin, W., Zha, Q. J., Guo, H. H., Zhang, D. D., Yang, L. P., Li, L., Li, D. P., & Tang, R. 2020. Persistent exposure to environmental levels of microcystin-lr disturbs cortisol production via hypothalamic-pituitary-interrenal (HPI) axis and subsequently liver glucose metabolism in adult male zebrafish (Danio rerio). Toxins. 12 (5), 282. https://doi.org/10.3390/toxins12050282
38. Willner, P., Muscat, R., & Papp, M. 1992. Chronic mild stress-induced anhedonia: a realistic animal model of depression. Neurosci Biobehav R. 16 (4), 525-534. https://doi.org/10.1016/s0149-7634(05)80194-0
39. Wu, S. T., Nguyen, L. T. M., Pan, H. R., Hassan, S., Dai, Y. M., Xu, J., & Wen, Z. L. 2020. Two phenotypically and functionally distinct microglial populations in adult zebrafish. Sci Adv. 6 (47), 1160. https://doi.org/10.1126/sciadv.abd1160
40. Yu, B., Zhang, D., Wu, Y., Tao, W., Luorong, Q., Luo, J., Tan, L., Chen, H., & Cao, W. 2023. A new polysaccharide from Hawk tea: Structural characterization and immunomodulatory activity associated with regulating gut microbiota. Food Chem. 418, 135917. https://doi.org/10.1016/j.foodchem.2023.135917
41. Zeng, J., Ji, Y., Luan, F., Hu, J., Rui, Y., Liu, Y., Rao, Z., Liu, R., & Zeng, N. 2022. Xiaoyaosan ethyl acetate fraction alleviates depression-like behaviors in CUMS mice by promoting hippocampal neurogenesis via modulating the IGF-1Rbeta/PI3K/Akt signaling pathway. J Ethnopharmacol. 288, 115005. https://doi.org/10.1016/j.jep.2022.115005
42. Zhang, Y. Y., Sun, Y., Liu, Y. P., Liu, J. M., Sun, J., Bai, Y. J., Fan, B., Lu, C., & Wang, F. Z. 2023. Polygonum sibiricum polysaccharides alleviate chronic unpredictable mild stress-induced depressive-like behaviors by regulating the gut microbiota composition and SCFAs levels. J Funct Foods. 101. https://doi.org/10.1016/j.jff.2023.105411
43. Zhang, Y. Y., Sun, Y., Liu, Y. P., Liu, J. M., Sun, J., Liu, X. M., Fan, B., Lu, C., & Wang, F. Z. 2023. Polygonum sibiricum polysaccharides exert the antidepressant-like effects in chronic unpredictable mild stress-induced depressive mice by modulating microbiota-gut-brain axis. Phytother Res. 37 (8), 3408-3423. https://doi.org/10.1002/ptr.7813
44. Zhao, L. P., Zhang, B. P., Huang, S. B., Zhou, Z. L., Jia, X. B., Qiao, C. M., Wang, F., Sun, M. F., Shi, Y., Yao, L., Cui, C., & Shen, Y. Q. 2022. Insulin-like growth factor-1 enhances motoneuron survival and inhibits neuroinflammation after spinal cord transection in zebrafish. Cell Mol Neurobiol. 42 (5), 1373-1384. https://doi.org/10.1007/s10571-020-01022-x
45. Zhao, P., Li, X., Wang, Y., Yan, L., Guo, L., Huang, L., & Gao, W. 2020. Characterisation and saccharide mapping of polysaccharides from four common Polygonatum spp. Carbohyd Polym. 233, 115836. https://doi.org/10.1016/j.carbpol.2020.115836
46. Zhu, R., Zhang, X., Wang, Y., Zhang, L., Zhao, J., Chen, G., Fan, J., Jia, Y., Yan, F., & Ning, C. 2019. Characterization of polysaccharide fractions from fruit of Actinidia arguta and assessment of their antioxidant and antiglycated activities. Carbohyd Polym. 210, 73-84. https://doi.org/10.1016/j.carbpol.2019.01.037